

# Facet braiding: a fundamental problem in integral imaging

R. Martínez-Cuenca, G. Saavedra, and A. Pons

Department of Optics, University of Valencia, E46100 Burjassot, Spain

B. Javidi

Electrical and Computer Engineering Department, University of Connecticut, Storrs, Connecticut 06269-1157, USA

M. Martínez-Corral

Department of Optics, University of Valencia, E46100 Burjassot, Spain

Received November 22, 2006; revised February 1, 2007; accepted February 8, 2007;  
posted February 12, 2007 (Doc. ID 77332); published April 3, 2007

A rigorous explanation of a phenomenon that produces significant distortions in the three-dimensional images produced by integral imaging systems is provided. The phenomenon, which we refer to as the facet-braiding effect, has been recognized in some previous publications, but to our knowledge its nature has never been analyzed. We propose a technique for attenuating the facet-braiding effect. We have conducted experiments to illustrate the consequences of the facet-braiding effect on three-dimensional integral images, and we show the usefulness of the proposed technique in eliminating this effect. © 2007 Optical Society of America

OCIS codes: 110.6880, 110.4190, 120.2040.

One of the challenges for the information society is the development, and the subsequent broad implementation, of technologies for the acquisition and display of three-dimensional (3D) pictures and movies. The search for the optimum 3D imaging/display technique has been the aim of research efforts for a long time.<sup>1</sup> However, only in the past few years has the technology reached the level required for the realization of this type of system. Among the existing 3D imaging techniques, the one known as integral imaging (InI) is especially appreciated because it has the ability to provide real or virtual autostereoscopic intensity images with full parallax. In an InI system the perspective information of a 3D scene is stored in a collection of 2D images, called elemental images, usually arranged in a rectangular grid. The main advantage of an InI monitor is the fact that one observer can see different perspectives of a 3D scene by simply varying his/her head position.<sup>2</sup>

InI was first proposed by Lippmann approximately one century ago.<sup>3</sup> Interest in InI has recently been resurrected because of its application to 3D TV.<sup>4</sup> A comprehensive introduction to InI can be found in Ref. 5. Although it is an attractive concept, the first designs of InI systems suffered from many problems. Consequently, much research has been focused on tackling, satisfactorily in many cases, such problems. For example, efforts have been made to improve the lateral resolution,<sup>6–8</sup> to enhance the depth-of-field<sup>9,10</sup> (DOF), for pseudoscopic to orthoscopic conversion,<sup>4,11,12</sup> and to minimize the elemental-image overlap.<sup>13</sup> InI systems have been shown to be useful not only for pure 3D imaging but also for other applications such as object recognition<sup>14</sup> and the mapping of 3D polarization distributions.<sup>15</sup>

There exists, however, a fundamental problem in InI that, although recognized in some publi-

cations,<sup>10,16,17</sup> has never been rigorously analyzed and described. We refer to the distortions suffered by out-of-focus scenes in a reconstruction that is visualized by observers. This effect, which impoverishes the quality of out-of-focus images, results from the braiding of visual facets. As a consequence of the facet-braiding effect, the effective DOF of the reconstructed images significantly decreases, even in the ideal case in which the pickup is realized with infinite DOF.

To get an intuitive understanding of the nature of the facet-braiding phenomenon, we start by drawing a scheme of the pickup stage of an InI system. As shown in Fig. 1, an object placed at the reference plane produces a collection of elemental images, all

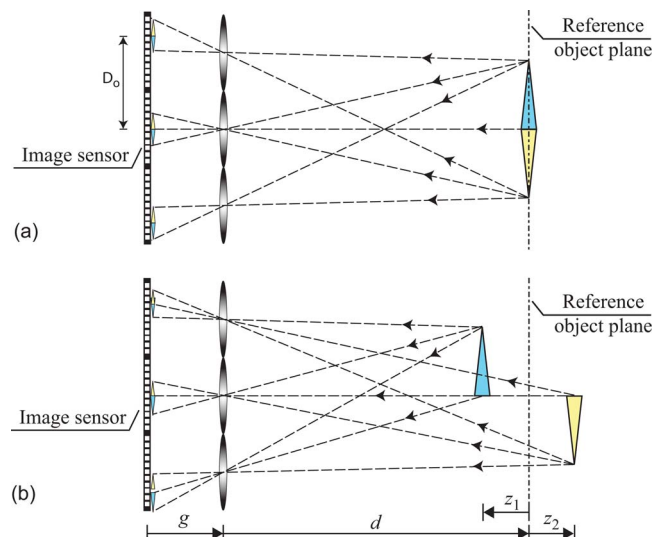


Fig. 1. (Color online) Schematic of the pickup stage of an InI system: elemental images of (a) an in-focus object and (b) out-of-focus scenes.

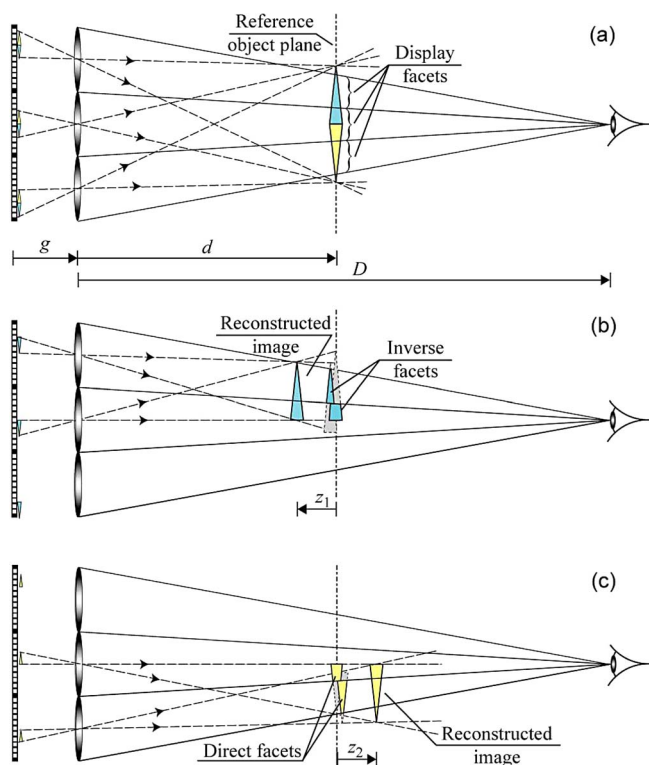


Fig. 2. (Color online) Display stage of an InI system. (a) Reconstructed images and the lenslet images coincide in position and size. (b) Images reconstructed between the MLA and the reference plane suffer inverse displacement. (c) Images further from the reference plane suffer direct displacement.

scaled by  $M_o = -g/d$  and separated by  $\Delta_o = p(1 - M_o)$ ,  $p$  being the pitch of the microlens array (MLA). In the case of out-of-focus objects the scale,  $M_i$ , the spacing, and the position of the elemental images depend on the distance between the object and the MLA, where  $M_i = -g/(d+z_i)$  and  $\Delta_i = p(1 - M_i)$ . Of course, the light emanating from out-of-focus points does not focus sharply onto the sensor. We will assume, however, that techniques for DOF enlargement are applied, so that even out-of-focus objects are recorded sharply.

Next, in Fig. 2 we schematize the reconstruction and visualization process. This process is the result of three phenomena: a geometrical projection, an image formation process, and finally, the arrangement of the visual facets.<sup>18</sup> As shown in Fig. 2(a), in the case of in-focus objects, a full consonance among the three phenomena occurs. (i) The rays emanating from the elemental images and passing through the center of the microlenses intersect at the reference plane so that the image is reconstructed with the same position and size as the object; (ii) the matrix sensor and the reference image plane are conjugate through the microlenses, thus implying that the images generated by each elemental image through the corresponding microlens coincide in size and position; (iii) when the observer places the eye in front of the MLA and looks through it, he/she observes a different portion of the reconstructed image through each microlens. Such image portions are referred to as visual facets. In this case the 3D image is seen with continuous relief, as shown in Fig. 3(a).

In the case of out-of-focus objects the consonance is broken, as shown in Figs. 2(b) and 2(c). (i) The image is reconstructed again with the same position and size as the object. (ii) The pickup device and the reference image plane are still conjugate through the microlenses. Therefore, the images generated by any elemental image through the corresponding microlens do not appear in the same position as the reconstructed image but appear in the reference plane instead. Although all of these images still have the same size, they appear centered at different positions. (iii) In the observation stage, the observer sees through each microlens one portion of the image provided by that particular microlens. But now the images provided by the microlenses are displaced so that the visual facets are arranged in a cracked relief. The cracking follows a braiding path. For scenes placed between the MLA and the reference plane, the images provided by the microlenses suffer an inverse displacement. To understand the concept of inverse displacement, refer to Fig. 3. In a given facet the corresponding part of the scene does not appear (as in the in-focus case). The scene is displaced towards the axis defined by the line of sight. Then in the facet a lower part of the image appears. For scenes farther than the reference plane the displacement is direct. This braidlike structure of the images produces a conflict in the visual-facets arrangement.

To illustrate the importance of the facet-braiding phenomenon we performed an experiment in which we obtained a set of  $39 \times 25$  elemental images of a 3D scene consisting of two capital letters, namely, H and S, each one printed on a different plate and located at distances 40 and 80 mm from the MLA, respectively. Note that the microlenses were square, with dimensions  $1.01 \text{ mm} \times 1.01 \text{ mm}$  and with a focal length of 3.30 mm. The pickup system was adjusted so that the reference plane was set at  $d = 35 \text{ mm}$ . In Fig. 4 we show three elemental images, which are elements of the same row of the elemental-image collection. Although the letter S was located 45 mm away from the

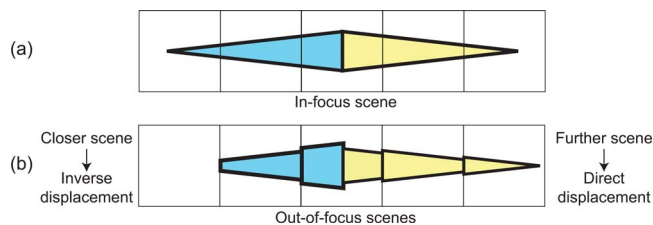


Fig. 3. (Color online) Structure of the observed reconstructed image, (a) Objects at the reference plane are seen with continuous relief. (b) Out-of-focus scenes are observed with cracked relief.



Fig. 4. (Color online) Three elements of the same row of the elemental-image collection.

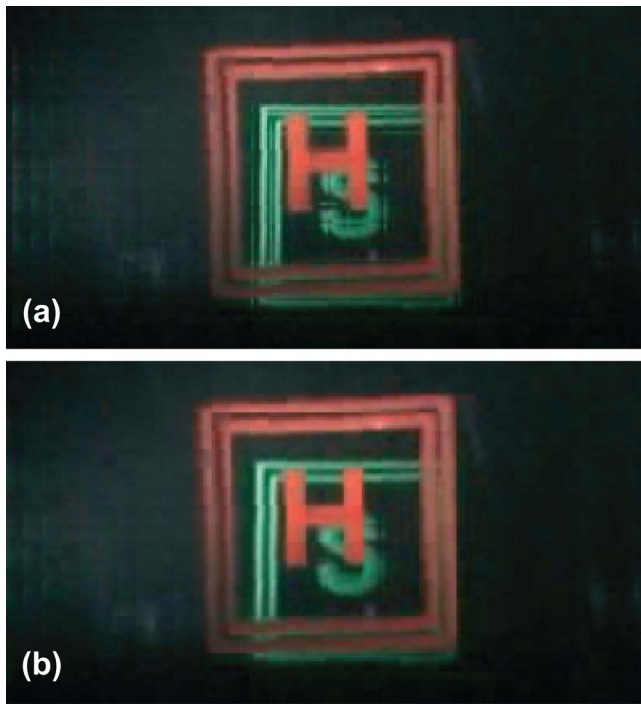


Fig. 5. (Color online) Views of the reconstructed 3D scene. (a) The reference plane was set, as in the pickup, at  $d = 35$  mm. (b) The reference plane for reconstruction was set at  $d = 52$  mm.

in-focus plane, it was recorded sharply because we fixed a high value for the  $f_{\#}$  ( $f_{\#} = 14$ ) of the macro objective used as the relay system for the capture.

We simulated the display stage by computer processing. In our calculations we assumed the same MLA as in the pickup, and that the observer was placed at a distance of  $D = 650$  mm from the MLA. We used the algorithm of Okano *et al.*<sup>4</sup> to reconstruct virtual orthoscopic images. In Fig. 5(a) we show a view of the reconstructed image. It is clear from the figure that only the in-focus letter H is observed without distortions. In the letter S, a direct facet-braiding effect is recognized, which produces a distortion that impoverishes the quality of both the letter and the square frame surrounding the letter.

To solve this problem we propose the use of a dynamic focusing technique during the display stage. The simplest solution for dynamic focusing is to control the gap between the display device and the MLA. However, this procedure suffers from the problem that a change in the gap inherently results in a change in the axial scale of the reconstructed images. Our proposal is not so simple, but instead it is much more exciting from a technological point of view. We propose the use of MLAs in which all the microlenses have the same focal length at any one time, but the focal length can be varied from one experiment to another. This type of MLA is not available yet, but the technology for their manufacture has already been demonstrated.<sup>19,20</sup> So we have simulated the reconstruction stage for a new value of the microlens focal length, namely,  $f = 3.20$  mm. This allows us to displace the reference image plane to  $d = 52$  mm. In Fig. 5(b) we show the view corresponding to the new re-

construction stage. Note how the dynamic focusing permits the selection of the plane free from the facet-braiding effect. Now the letter S is observed with continuous relief. The cracking inherent to direct braiding has disappeared.

To conclude, we have reported a rigorous explanation of a fundamental problem that usually impoverishes the performance of InI systems. Let us remark that in case of InI reconstruction working in the depth priority regime the facet-braiding effect is more intense. This is because in such a case the distance between the reference image plane and the reconstructed image is infinity. The thorough understanding of the nature of the facet-braiding phenomenon allowed us to suggest a solution for this problem. Of course the proposed technique is effective only in a limited range of axial distances in the neighborhood of the reference image plane. Thus, the position of such a plane should be selected carefully. We have performed a hybrid experiment that shows the usefulness of our technique.

This work has been funded in part by the Plan Nacional I+D+I (grant DPI2006-8309), Ministerio de Educación y Ciencia, Spain. R. Martínez-Cuenca acknowledges funding from the Universitat de València (Cine Segles grant). We also acknowledge the support from the Generalitat Valenciana (grant GV06/219). M. Martínez-Corral's e-mail address is manuel.martinez@uv.es.

## References

1. T. Okoshi, Proc. IEEE **68**, 548 (1980).
2. F. Okano, Proc. IEEE **94**, 490 (2006).
3. M. G. Lippmann, J. Phys. (Paris) **7**, 821 (1908).
4. F. Okano, H. Hoshino, J. Arai, and I. Yayuma, Appl. Opt. **36**, 1598 (1997).
5. A. Stern and B. Javidi, Proc. IEEE **94**, 591 (2006).
6. A. Stern and B. Javidi, Appl. Opt. **42**, 7036 (2003).
7. S. Manolache, A. Aggoun, M. McCormick, and N. Davies, J. Opt. Soc. Am. A **18**, 1814 (2001).
8. J.-S. Jang and B. Javidi, Opt. Lett. **27**, 324 (2002).
9. R. Martínez-Cuenca, G. Saavedra, M. Martínez-Corral, and B. Javidi, Opt. Express **12**, 5237 (2004).
10. B. Lee, S.-W. Min, and B. Javidi, Appl. Opt. **41**, 4856 (2002).
11. N. Davies, M. McCormick, and L. Yang, Appl. Opt. **27**, 4520 (1988).
12. M. Martínez-Corral, B. Javidi, R. Martínez-Cuenca, and G. Saavedra, Opt. Express **13**, 9175 (2005).
13. R. Martínez-Cuenca, A. Pons, G. Saavedra, M. Martínez-Corral, and B. Javidi, Opt. Express **14**, 9657 (2006).
14. Y. Frauel, O. Matoba, E. Tajahuerce, and B. Javidi, Appl. Opt. **43**, 452 (2004).
15. O. Matoba and B. Javidi, Opt. Lett. **29**, 2375 (2004).
16. Y. Kim, J.-H. Park, H. Choi, J. Kim, S.-W. Cho, and B. Lee, Appl. Opt. **45**, 4334 (2006).
17. T. Naemura, T. Yoshida, and H. Harashima, Opt. Express **8**, 255 (2001).
18. M. Martínez-Corral, B. Javidi, R. Martínez-Cuenca, and G. Saavedra, J. Opt. Soc. Am. A **22**, 597 (2005).
19. C.-C. Cheng, C. Alex Chang, and J. A. Yeh, Opt. Express **14**, 4101 (2006).
20. L. Dong, A. K. Agarwal, D. J. Beebe, and H. Jiang, Nature **442/3**, 551 (2006).